Supplementary material

Facile One-step Hydrothermal Synthesis of α-Fe_2O_3/g-C_3N_4 Composites for the Synergistic Adsorption and Photodegradation of Dyes

Tao Wang[a, b], Manqi Huang[a, b], Xiawei Liu[a, b], Zhen Zhang[c], Yonghong Liu[c], Wei Tang[a], Shaopan Bao[a], Tao Fang[a, b, *]

[a] *Institute of Hydrobiology, Chinese Academy of Sciences, Wuhan 430072, China*

[b] *University of Chinese Academy of Sciences, Beijing 100049, China*

[c] *College of Science, Huazhong Agricultural University, Wuhan 430070, China*

[*] Corresponding author*:* Institute of Hydrobiology, Chinese Academy of Sciences, 7 Donghu South Road, Wuchang District, Wuhan 430072, China.

E-mail address: fangt@ihb.ac.cn (T. Fang).

Table S1 Porous structure parameters of as-prepared sample.

Samples	BET Surface Area ($m^2 g^{-1}$)	Total pore volume ($cm^3 g^{-1}$)	Average pore width (nm)
g-C_3N_4	69.6	0.15	8.54
a-Fe_2O_3/g-C_3N_4-0.25	55.0	0.13	9.57
a-Fe_2O_3/g-C_3N_4-0.5	52.2	0.14	10.55
a-Fe_2O_3/g-C_3N_4-1	45.4	0.11	9.85

Table S2 Comparison of maximum adsorption capacity of MO and MB on g-C_3N_4, α-Fe_2O_3/g-C_3N_4-0.5 and other adsorbents.

Species	Materials	pH	q_{max} (mg g^{-1})	Ref
MO	MPC-300	5.0	25.52	[1]
	De-Oiled Soya	3.0	16.66	[2]
	Spent tea leaves (STL) modified with PEI	3.0	62.11	[3]
	g-C_3N_4	3.0	34.61	This work
	α-Fe_2O_3/g-C_3N_4-0.5	3.0	**69.91**	This work
MB	Marine seaweed	5.0	5.20	[4]
	Wheat shells	7.0	16.56	[5]
	Activated carbon	7.0	9.81	[6]
	g-C_3N_4	8.0	9.66	This work
	α-Fe_2O_3/g-C_3N_4-0.5	8.0	**29.46**	This work

Text S1 Isotherms model for the adsorption

The Langmuir isotherm was used to describe the monolayer of adsorbate on the adsorbent surface and the surface homogeneity of the adsorbent. The Langmuir equation could be expressed as equation (S1) [7]:

$$q_e = \frac{q_{max} C_e b}{1 + C_e b} \quad \text{(S1)}$$

The Freundlich model indicates the multilayer adsorption and the surface heterogeneity of the adsorbent. The Freundlich isotherm could be given as equation (S2) [8]:

$$q_e = K_f C_e^{1/n} \quad \text{(S2)}$$

where C_e (mg L^{-1}) denotes the equilibrium concentration, q_{max} (mg g^{-1}) expresses the maximum theoretical saturated adsorption capacity, b (L mg^{-1}) denotes the

Langmuir adsorption constant, K_f (mg^{1-n} L^n g^{-1}) is the Freundlich adsorption coefficient and n is the constant depicting the adsorption intensity.

Text S2 Kinetics model for the adsorption

The pseudo-first-order kinetic model is described as equation (S3) [7]:

$$\ln\left(q_e - q_t\right) = \ln q_e - k_1 t \qquad \text{(S3)}$$

The pseudo-second-order kinetic model is described as equation (S4) [9]:

$$\frac{t}{q_t} = \frac{1}{k_2 q_e^2} + \frac{t}{q_e} \qquad \text{(S4)}$$

where k_1 and k_2 represent the pseudo-first- and pseudo-second-order rate constants, q_e and q_t (mg g^{-1}) denote the adsorption of MO/MB at equilibrium and time t (min)

Table S3. Kinetic parameters for the adsorption of MO and MB on α-Fe_2O_3/g-C_3N_4-0.5.

		Pseudo-first-order			Pseudo-second-order		
species	$q_{e,exp}$ (mg g^{-1})	$q_{e,cal}$ (mg g^{-1})	k_1 (1 min^{-1})	R^2	$q_{e,cal}$ (mg g^{-1})	k_2 (g mg^{-1} min^{-1} 10^3)	R^2
MO	69.08	16.39	0.011	0.873	70.47	1.830	1
MB	22.64	4.96	0.010	0.854	24.40	4.320	0.998

Text S3 Thermodynamic adsorption analysis

The standard free energy change (ΔG^0) can be calculated from the following equation (S5) [10]:

$$\Delta G^0 = -RT\ln K^0 \qquad \text{(S5)}$$

where R is the universal gas constant (8.314 J $mol^{-1}K^{-1}$), T is the temperature in Kelvin. The sorption equilibrium constant, K^0, can be calculated by plotting $\ln K_d$ versus C_e (Figures S4) and extrapolating C_e to zero. The standard enthalpy change (ΔH^0) and the standard entropy change (ΔS^0) are calculated from the following equation (S6) [10]:

$$\ln K^0 = \frac{\Delta S^0}{R} - \frac{\Delta H^0}{RT} \qquad \text{(S6)}$$

Linear plots of $\ln K^0$ vs 1/T for MO and MB adsorption on α-Fe_2O_3/g-C_3N_4-0.5 are shown in Figure S5. The thermodynamic parameters are calculated from the plot of $\ln K^0$ vs 1/T using equations (S5) and (S6).

Table S4. Thermodynamics parameters for the adsorption of MO and MB on α-Fe_2O_3/g-C_3N_4-0.5.

			ΔG^0 (kJ mol^{-1})		
species	ΔH^0 (kJ mol^{-1})	ΔS^0 (J mol^{-1} k^{-1})	298K	308K	318K
MO	-17.84	-33.65	-7.89	-7.32	-7.23
MB	6.72	51.68	-8.69	-9.18	-9.73

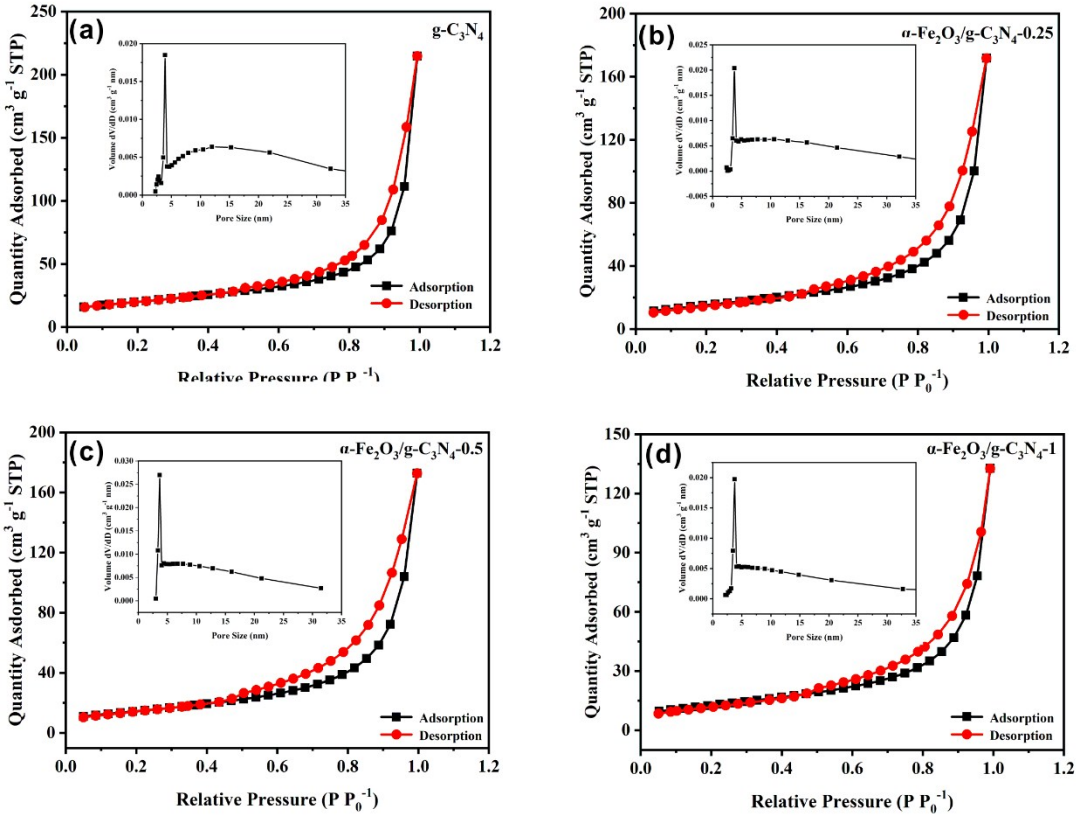

Fig. S1. N_2 adsorption-desorption isotherms and pore size distributions of as-prepared samples.

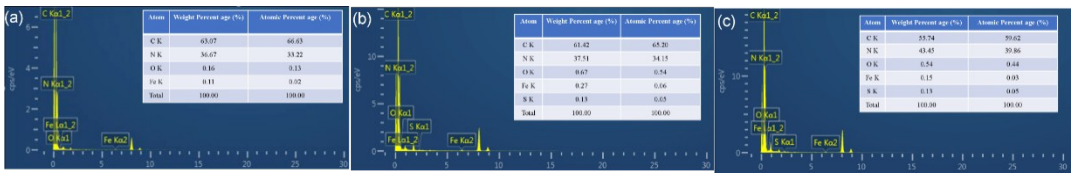

Fig. S2. EDS images on α-Fe_2O_3/g-C3N4-0.5 before adsorption (a), after MO adsorption (b) and after MB adsorption (c).

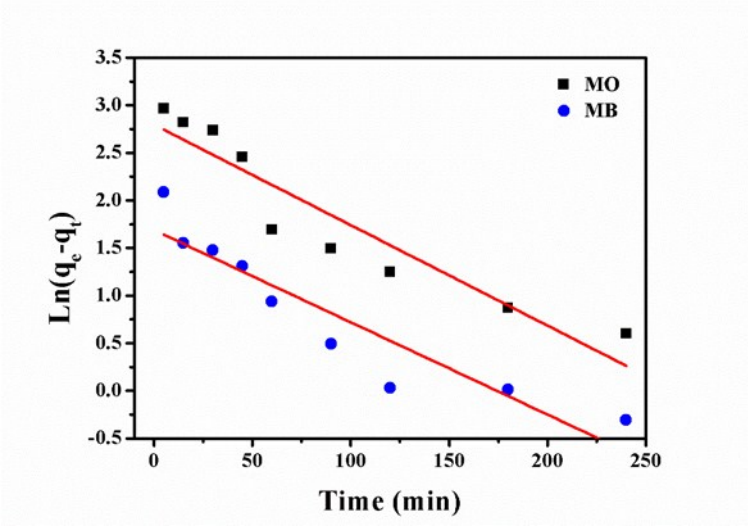

Fig. S3. Pseudo-first-order linear plots for the removal of MO/MB by α-Fe_2O_3/g-C_3N_4-0.5. pH_{MO} = 3.0 ± 0.1, pH_{MB}= 8.0± 0.1, m/V = 0.25 g L^{-1}, and T = 298 ± 1 K.

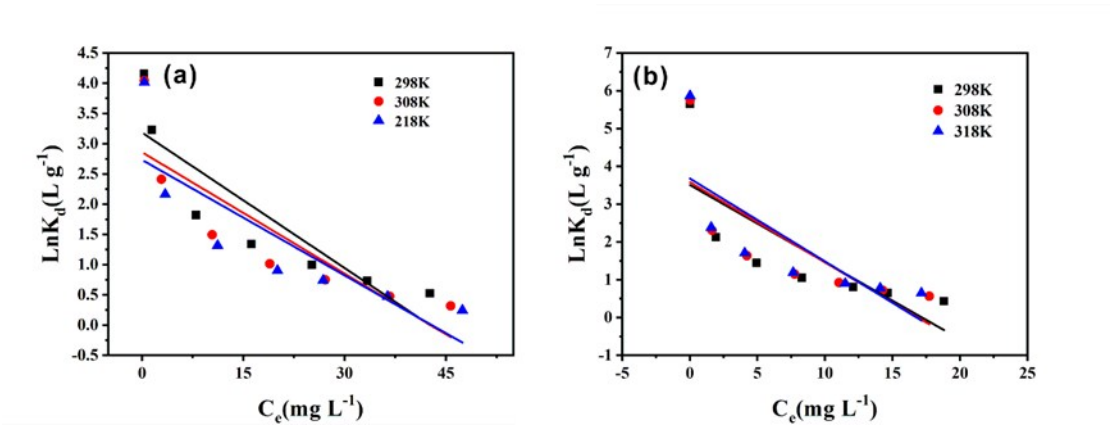

Fig. S4. Linear plots of lnK_d vs C_e for MO (a) and MB (b) adsorption on α-Fe_2O_3/g-C_3N_4-0.5 at 298, 308, and 318 K. pH_{MO} = 3.0 ± 0.1, pH_{MB}= 8.0± 0.1, and m/V = 0.25 g L^{-1}.

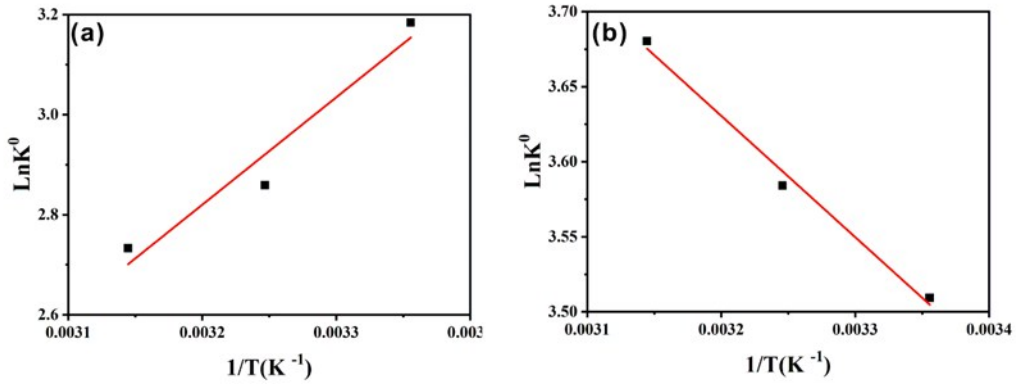

Fig. S5. Linear plots of $\ln K^0$ vs 1/T for the adsorption of MO (a) and MB (b) on α-Fe_2O_3/g-C_3N_4-0.5 at 298, 308, and 318 K. pH_{MO} = 3.0 ± 0.1, pH_{MB}= 8.0± 0.1, and m/V = 0.25 g L^{-1}.

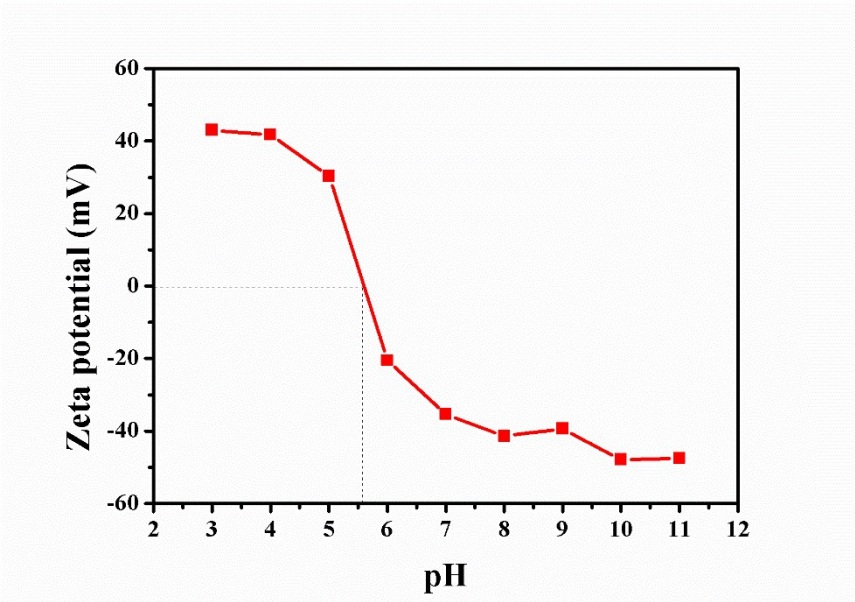

Fig. S6. Zeta-potential of the α-Fe_2O_3/g-C_3N_4-0.5 as a function of pH value.

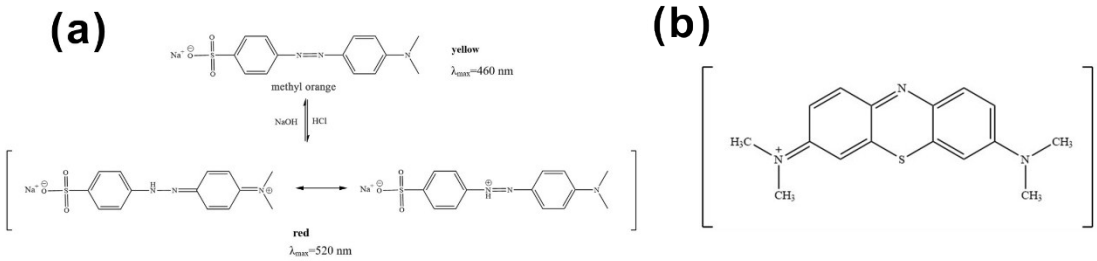

Fig. S7. The chemical structures of (a) methyl orange molecule in basic solution and the canonical forms in acidic solution [3], (b) methylene blue.

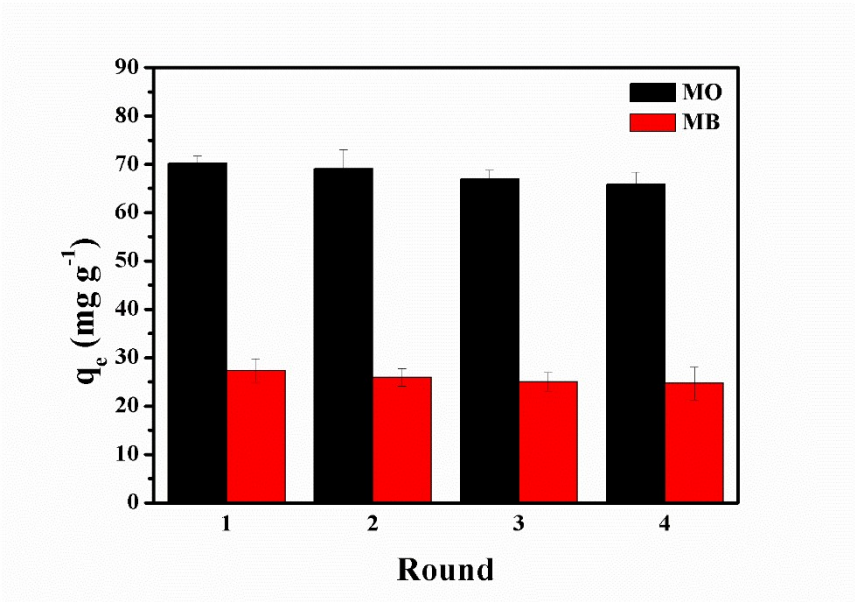

Fig. S8. Recycling of α-Fe_2O_3/g-C_3N_4-0.5 in the removal of MO/MB. pH_{MO} = 3.0 ± 0.1, pH_{MB}= 8.0± 0.1, m/V = 0.25 g L^{-1}, and T = 298 ± 1 K.

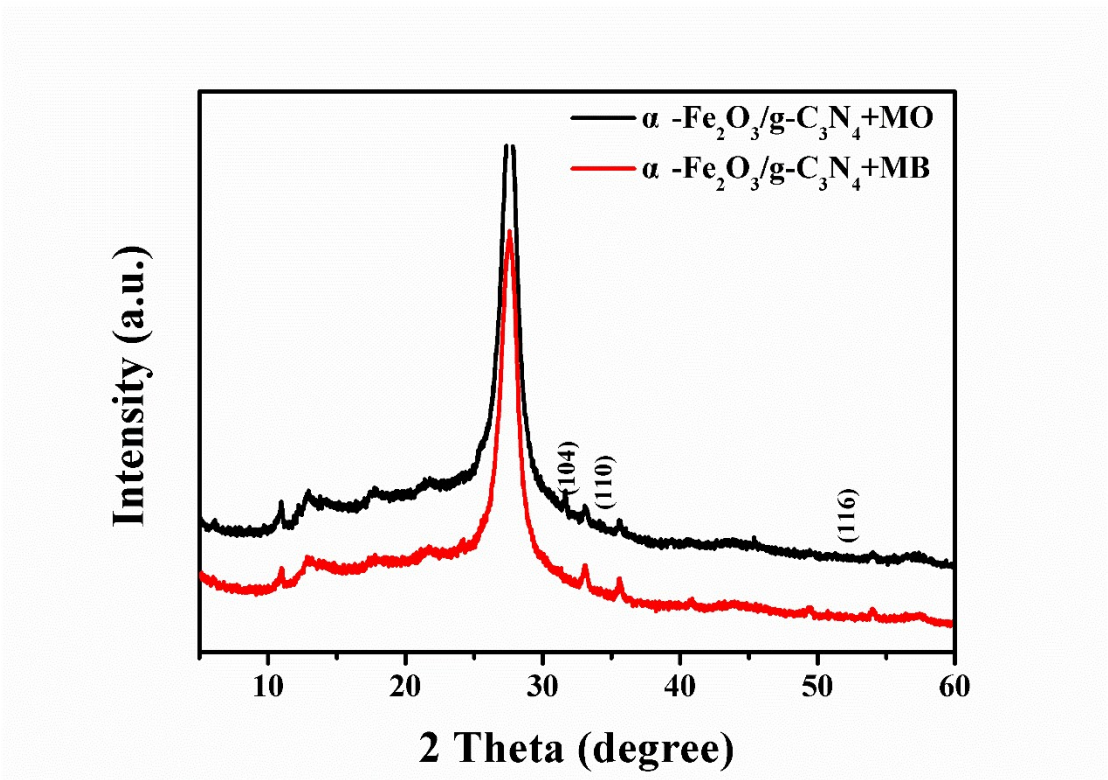

Fig. S9. XRD patterns on α-Fe_2O_3/g-C3N4-0.5 after MO/MB adsorption and photocatalytic degradation

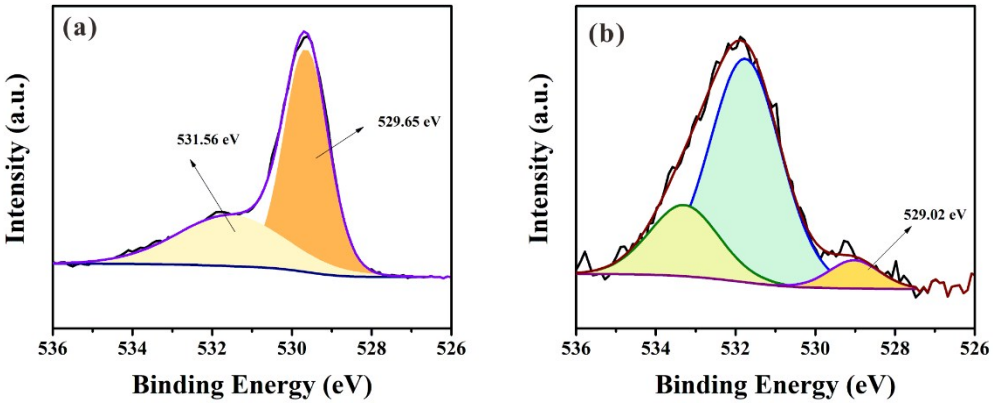

Fig. S10. XPS image α-Fe_2O_3/g-C_3N_4-0.5 (a) O 1s and α-Fe_2O_3 (b) O 1s.

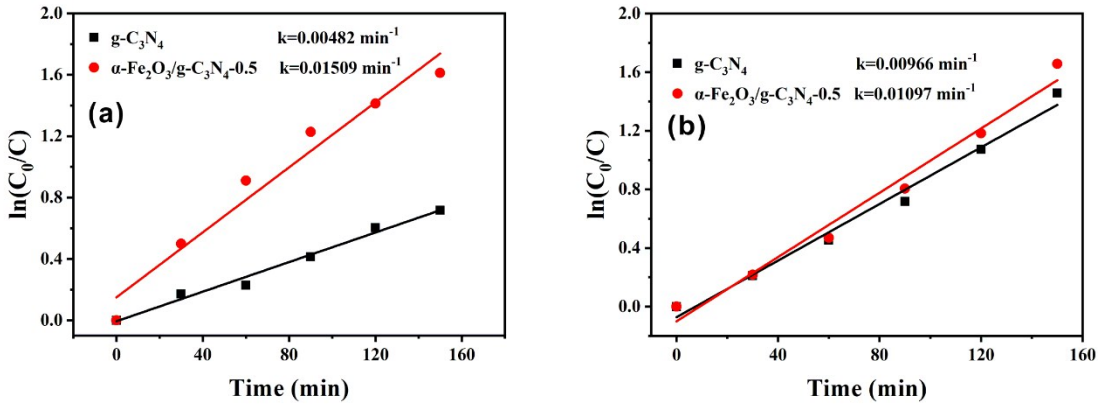

Fig. S11. Kinetic fit of the photoreduction of MO (a) and MB (b) by g-C_3N_4, and α-Fe_2O_3/g-C_3N_4-0.5, respectively, to the first-order kinetic model under visible light irradiation (□≥420 nm). pH_{MO} = 3.0 ± 0.1, pH_{MB}= 8.0± 0.1, m/V = 0.25 g L^{-1}, and T = 298 ± 1 K.

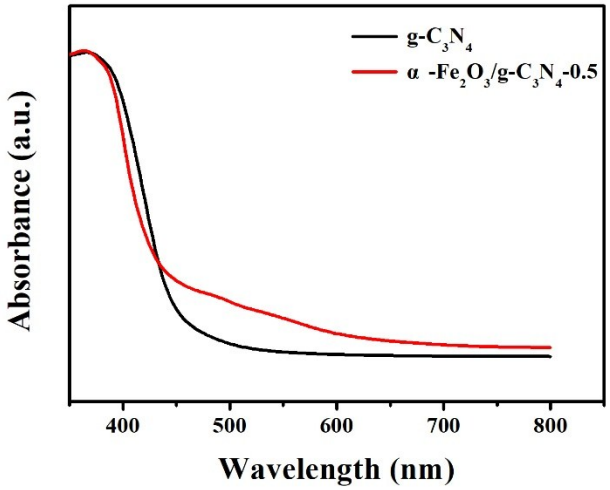

Fig. S12. UV–vis spectra of g-C_3N_4 and α-Fe_2O_3/g-C_3N_4-0.5.

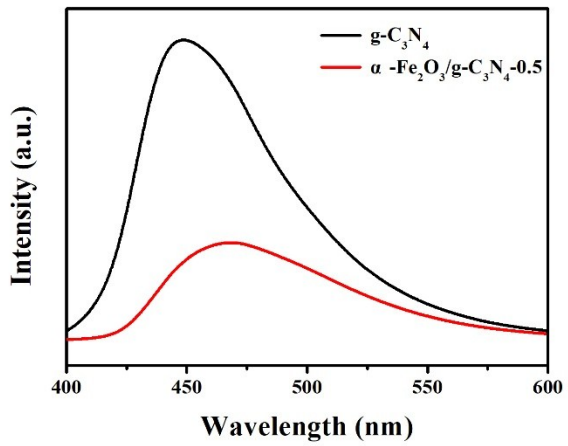

Fig. S13. PL spectra of g-C_3N_4 and α-Fe_2O_3/g-C_3N_4-0.5

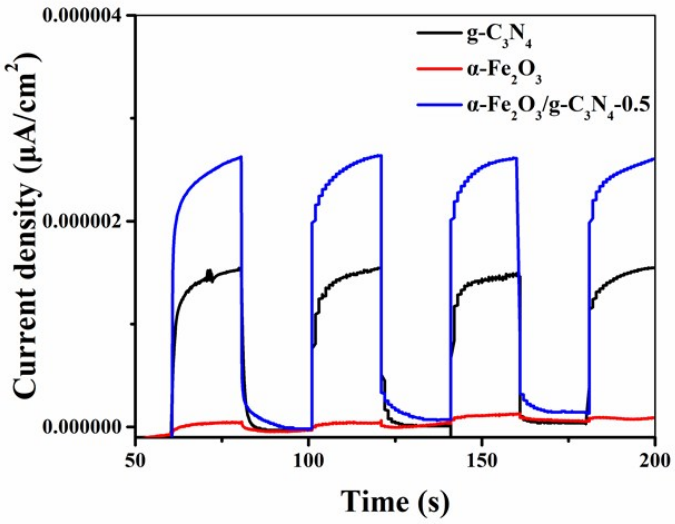

Fig. S14. Time-current curves of α-Fe_2O_3, g-C_3N_4, and α-Fe_2O_3/g-C_3N_4-0.5.

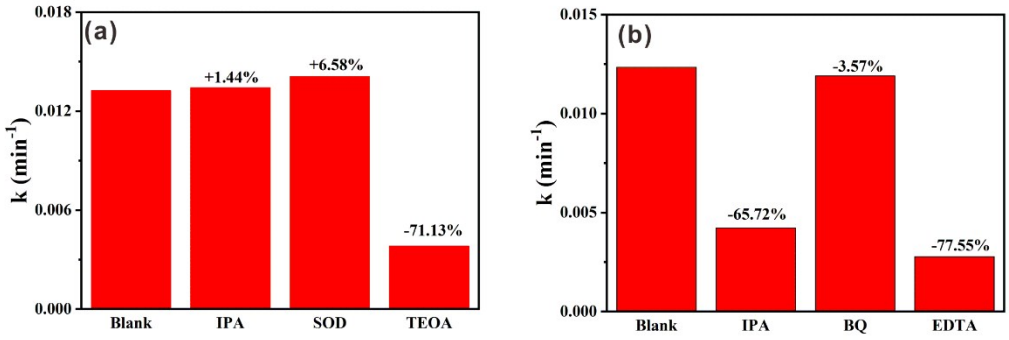

Fig. S15. Kinetic constants for photocatalytic degradation of MO (a) and MB (b) over α-Fe_2O_3/g-C_3N_4-0.5 at different scavengers (IPA, 0.01ml; TEOA, 0.01ml; SOD/TEOA, 1mg). pH_{MO} = 3.0 ± 0.1, pH_{MB}= 8.0± 0.1, m/V = 0.25 g L^{-1}, and T = 298 ± 1 K.

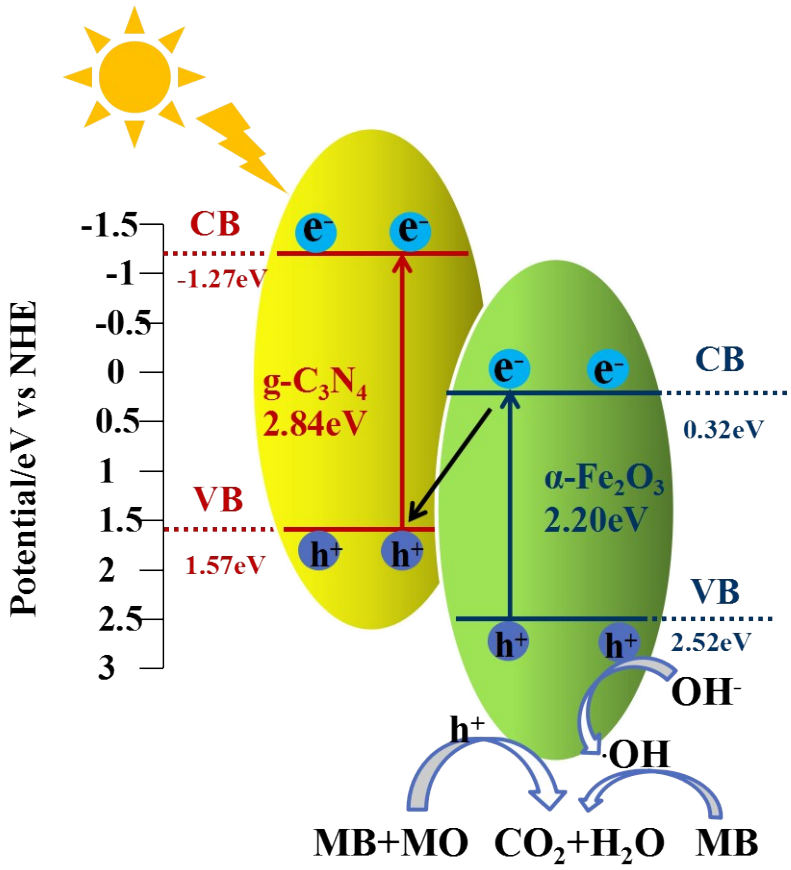

Fig. S16. Possible photocatalytic degradation mechanism of MO/MB over the α-Fe_2O_3/g-C_3N_4-0.5.

References

1. T. Wen, J. Wang, S. Yu, Z. Chen, T. Hayat and X. Wang, *ACS Sustainable Chemistry &*

Engineering, 2017, **5**, 4371-4380.

2. A. Mittal, A. Malviya, D. Kaur, J. Mittal and L. Kurup, *J Hazard Mater*, 2007, **148**, 229-240.
3. S. Wong, H. H. Tumari, N. Ngadi, N. B. Mohamed, O. Hassan, R. Mat and N. A. Saidina Amin, *Journal of Cleaner Production*, 2019, **206**, 394-406.
4. S. Cengiz and L. Cavas, *Bioresource Technol*, 2008, **99**, 2357-2363.
5. Y. Bulut and H. Aydin, *Desalination*, 2006, **194**, 259-267.
6. V. V. B. Rao and S. R. M. Rao, *Chemical Engineering Journal*, 2006, **116**, 77-84.
7. J. Wang, P. Wang, H. Wang, J. Dong, W. Chen, X. Wang, S. Wang, T. Hayat, A. Alsaedi and X. Wang, *ACS Sustainable Chemistry & Engineering*, 2017, **5**, 7165-7174.
8. K. W. Jung, S. Y. Lee and Y. J. Lee, *Bioresour Technol*, 2018, **261**, 1-9.
9. X. Q. Liu, H. S. Ding, Y. Y. Wang, W. J. Liu and H. Jiang, *Environ Sci Technol*, 2016, **50**, 2602-2609.
10. G. X. Zhao, J. X. Li, X. M. Ren, C. L. Chen and X. K. Wang, *Environmental Science & Technology*, 2011, **45**, 10454-10462.